EAGLE INTERNATIONAL JOURNAL OF SCIENCE, TECHNOLOGY AND INNOVATION [EIJSTI]

Eagle International Journal of Science, Technology and Innovation

An International Peer Reviewed, Open-Access and Multidisciplinary Journal
Volume 1 | Issue 2 | October 2026 |
Website: https://eijrihs.com/index.php/eijsti/index

OPTIMIZATION AND MICROSTRUCTURAL CHARACTERISTICS OF CONCRETE PRODUCED WITH PARTIAL REPLACEMENT OF ABUJA RIVER SAND WITH LATERITE

Abegunde Joseph Folorunso[1], Emmanuel E. Ndububa[2] , Blessing Ekwe[3]

1,2 Department of Civil Engineering, University of Abuja, Abuja, Nigeria

3 Department of Building, University of Abuja, Abuja, Nigeria

Corresponding Author: Abegunde Joseph Folorunso.
Email: folorunsoabegunde@yahoo.com

ABSTRACT

Sand dredging along rivers in the Federal Capital Territory (FCT), Nigeria, is damaging the environment and pushing up the price of fine aggregate, which has prompted interest in other sources of fine material. In this work, Abuja river sand in concrete was partly substituted with laterite from Lugbe (FCT) at 0–4% of the fine aggregate mass. A Scheffé {6, 3} simplex-lattice plan with six components (water, cement, river sand, laterite, superplasticizer and coarse aggregate) gave 56 mixtures, and each was tested in triplicate for compressive strength, flexural strength and slump flow. The laterite (SiO_2 ≈ 32%, Al_2O_3 ≈ 20%, and Fe_2O_3 ≈ 8%) was sandy clay with 14% clay, a specific gravity of 2.48 and 11.2% water absorption. Because a superplasticizer was used, slump flow stayed within 551–580 mm in every mixture. Mean compressive strength lay between 20.28 and 26.21 MPa, and mean flexural strength between 2.73 and 3.80 MPa. However, the variation among the three specimens of a mixture (coefficient of variation about 14%) was as big as the variation between mixtures, and an analysis of variance based on the replicates found no significant mixture effect on compressive strength ($p = 0.998$) or flexural strength ($p = 0.935$). SEM–EDS examination of four groups of mixtures revealed dense, calcium-silicate-hydrate-rich matrices and compact interfacial transition zones in the stronger groups, while the weaker groups showed more pores, broken hydration products and microcracks. Strengths of 20–26 MPa were achieved with up to 4% laterite in the fine aggregate. A larger replicated programme covering a wider replacement range is needed before any optimum replacement level can be stated.

KEYWORDS: *laterite; laterized concrete; river sand replacement; flexural strength; Scheffé simplex-lattice design; microstructure; sustainable construction.*

1. INTRODUCTION

Concrete is the construction material used in the greatest quantities worldwide, and the fine aggregate in it, most often natural river sand, has a strong bearing on workability, strength, durability and dimensional stability. Fast urban growth and infrastructure projects in Abuja have raised demand for river sand. Intensive extraction is linked to deepening of river beds, collapse of banks, disturbed sediment balance and damage to aquatic habitats and it has also made good-quality sand more expensive [1]. These problems have encouraged the use of locally available substitutes that lessen reliance on river sand while keeping structural performance acceptable.

Laterite is a residual tropical soil produced by long weathering under hot, wet conditions. It is rich in iron and aluminium oxides, usually has a silica-to-sesquioxide ratio below 1.33, and is plentiful in the FCT, where it has traditionally served in road bases, embankments, earthworks and masonry units. The use of laterite in place of sand in concrete, now called laterized concrete, was first studied by D. Adepegba [2], who advised replacing as much as about 25% of the sand with lateritic fines in a 1:1.5:3 mix. Subsequent studies looked at how sand content, laterite content, curing regime and mix proportions affect the strength, creep, flexural behaviour and durability of such concrete [3]–[8]. Replacement levels of roughly 10–25% have been reported to give strengths close to those of conventional concrete [9], [12], while strength falls at higher levels (above about 30%), a trend usually put down to the clay content and greater water demand of lateritic soils [10]. Laterized concrete is also generally less workable than ordinary concrete, since lateritic particles have a larger surface area and absorb more water [11], and the water–cement ratio strongly governs both its strength and its workability [13].

The effect of laterite on concrete is thus twofold. Fine lateritic particles can improve packing and make the paste and the interfacial transition zone (ITZ) denser, and their silica- and alumina-bearing phases may add a small contribution to secondary hydration. On the other hand, too much clay mineral soaks up mixing water, hinders cement hydration and weakens the bond between paste and aggregate, and the ITZ is already the weakest zone in concrete [14]. Since the composition of lateritic soils changes with parent rock, location and processing [15], findings from other regions cannot be carried over directly to Abuja materials.

Microstructural work on laterized systems has been published [16], [17], but most studies change only the laterite proportion and report compressive strength; few bring mechanical testing, microstructural study and statistical optimization together in one programme. Scheffé's simplex-lattice design [18] lets every component of a mixture be varied at once under the condition that the proportions add up to one, and it produces polynomial models that can predict properties and locate optimum proportions.

This paper presents a laboratory study of concrete in which Abuja river sand was partly replaced by laterite from Lugbe, FCT. The objectives were to (i) establish the physical and chemical properties of the river sand and laterite; (ii) assess how mixture composition, including laterite content, affects workability and compressive and flexural strength; (iii) fit third-degree Scheffé models and examine how useful they are for strength optimization; and (iv) study the concrete microstructure by SEM–EDS. The work is restricted to laboratory-scale specimens and covers fresh properties, strength and microstructure; long-term durability lies outside its scope.

2. MATERIALS AND METHODS

2.1 Materials

The cement was Dangote 3X Ordinary Portland cement (grade 42.5, conforming to ASTM C150 and BS EN 197-1), bought from a building-materials market in Lugbe, Abuja. River sand came from a construction site in Lugbe; it showed no visible organic matter or debris, and it was sieved through 2.36 mm and air-dried before use. Laterite was dug by hand at about 300 mm depth from a borrow pit in the Jiwa area of Lugbe (approximate coordinates 9.006474, 7.338667), a pit that supplies road-construction material. The soil was reddish-brown, fine-grained and became hard on drying, and boulders and lateritic gravel were screened out before use. The coarse aggregate was crushed granite of 4.75–20 mm nominal size, taken from a construction site in Lugbe. Potable water was used for mixing and curing. A high-range water-reducing admixture (Hydroplast 260GR; brown liquid, density 1.16 g/cm³, chloride-free to EN 934, pH 7–9) was added at 1.3–3.3% of the cement mass, following the batch quantities in Table A1.



Figure 1: (a) Laterite (b) Cement (c) Fine Aggregate (d) Coarse Aggregate

2.2 Characterization of materials

All material tests were done in the laboratory of the Nigerian Building and Road Research Institute (NBRRI), Jabi, Abuja. Particle-size distributions of the aggregates were obtained by dry sieving (ASTM C136; BS 812-103), and the coefficients of uniformity (Cu) and curvature (Cc) were computed from the grading curves:

$$C_u = D_{60} / D_{10} \quad (1)$$

$$C_c = (D_{30})^2 / (D_{10} \times D_{60}) \quad (2)$$

Where D_{10}, D_{30} and D_{60} are the particle sizes below which 10%, 30% and 60% of the material is finer. Specific gravity of the aggregates was determined by the Pycnometer method (ASTM C127, C128; BS 812-2; BS 1377-2):

$$G_s = (m_2 - m_1) / [(m_4 - m_1) - (m_3 - m_2)] \quad (3)$$

Where m1 is the mass of the empty bottle, m2 the bottle with dry aggregate, m3 the bottle with aggregate and water, and m4 the bottle filled with water. Natural moisture content and water absorption were also measured. Sand, silt and clay fractions of the laterite and river sand were found by sedimentation analysis (ASTM D422), the laterite was classified by the Unified Soil Classification System (USCS), and its oxide composition was determined by X-ray fluorescence (XRF).

2.3 Mixture design

A Scheffé simplex-lattice design [18] was applied with six components: water (X1), cement (X2), river sand (X3), laterite (X4), superplasticizer (X5) and coarse aggregate (X6). Their proportions are bound by:

$$X_1 + X_2 + X_3 + X_4 + X_5 + X_6 = 1, \quad 0 \le X_i \le 1 \quad (4)$$

The number of design points in a {q, m} simplex-lattice, with q components and a polynomial of degree m, is;

$$N = (q + m - 1)! / [m! (q - 1)!] \quad (5)$$

Which yields N = 56 for q = 6 and m = 3. Three specimens were cast for each mixture, so 168 specimens were tested for each property. Table A1 lists the batch quantities of the 56 mixtures (kg per batch); they ranged from 0.495–0.54 (water), 0.885–0.94 (cement), 2.38–2.44 (river sand), 0–0.1 (laterite), 0.012–0.03 (superplasticizer) and 2.78–2.87 (coarse aggregate). Laterite formed 0–4.0% of the fine aggregate by mass (mean 1.2%), so only low replacement levels are covered. Batch quantities were converted using these densities (kg/m³): water 1000, cement 1440, river sand 1714, laterite 1887, superplasticizer 1170 and coarse aggregate 2156.

2.4 Mixing, casting and curing

Materials were batched by mass and mixed by hand on a watertight, non-absorbent platform. Cement and the fine aggregates (river sand and laterite) were blended first, the coarse aggregate followed, and water containing the superplasticizer was added last until the mix looked uniform. Cubes of 150 mm (0.003375 m³) and prisms of 160 × 40 × 40 mm were cast in oiled moulds in layers of about 50 mm, each layer receiving 25 strokes of a 16 mm rod, and were removed from the moulds after 24 h. Curing was in potable water at about 24 °C until the test date.

2.5 Fresh and hardened concrete tests

Slump flow was measured to BS EN 12350-8 and compared with the EFNARC guideline range of 550–850 mm [19]; cohesion, bleeding and colour were also noted. Compressive strength was found on 150 mm cubes in a universal testing machine (ASTM C39/C39M; BS EN 12390-2) as the failure load P divided by the loaded area A:

$$\sigma = P / A \quad (6)$$

Flexural strength was found on 160 × 40 × 40 mm prisms under two-point loading (BS EN 12390-5) as :

$$f_{cr} = PL / (bd^2) \quad (7)$$

where P is the failure load, L the span, and b and d the breadth and depth of the prism. All strengths are given at 28 days as the mean of three specimens.

2.6 Microstructural analysis

Small fragments of hardened concrete were taken, dried and given a conductive coating before examination by scanning electron microscopy with energy-dispersive X-ray spectroscopy (SEM–EDS) at NBRRI. Four representative spots (Spots 1–4) were chosen to stand for groups of mixtures with progressively weaker laboratory performance, and the hydration products, pore structure, microcracks, ITZ and particle bonding were studied. XRD was also run on the laterite and on selected concrete samples in the same laboratory.

2.7 Statistical modelling and optimization

The mean compressive and flexural strengths of the 56 mixtures were fitted with Scheffé polynomials of the form;

$$Y = \Sigma\beta_i X_i + \Sigma\beta_{ij} X_i X_j + \Sigma\beta_{ijk} X_i X_j X_k + \Sigma\beta_{iij} X_i^2 X_j \quad (8)$$

Coefficients were estimated by regression in the Wolfram Language, using the mean strength of each mixture. As three specimens were tested per mixture, differences among mixtures were checked against the pure error of the replicates by one-way analysis of variance (ANOVA) at the 95% confidence level. The fitted polynomial was to be maximized under Equation 4, with lower and upper limits set at the smallest and largest observed responses.

3. RESULTS AND DISCUSSION

3.1 Characterization of the materials

3.1.1 Chemical composition of the laterite

The XRF results (Table 1) show a laterite made up mainly of silica (about 32%), alumina (about 20%) and iron oxide (about 8%), with about 6% magnesia and only traces of TiO_2, P_2O_5 and SO_3. This is typical of lateritic soil, where heavy leaching strips away soluble bases and leaves iron and aluminium oxides behind. The small SO_3 content is an advantage for durability, since sulphate-bearing aggregates can lead to sulphate attack. The silica and alumina suggest that the fine lateritic particles may act as a micro-filler and could show weak pozzolanic activity.

Table 1. Oxide composition of the laterite (XRF).

Oxide	Content (%)
SiO_2	≈ 32
Al_2O_3	≈ 20
Fe_2O_3	≈ 8
MgO	≈ 6
TiO_2, P_2O_5, SO_3	trace

3.1.2 Physical properties of the aggregates

The laterite is finer than the river sand (Table 2): its fineness modulus is 2.21 against 2.65 for the sand, and 72.8% of it passes the 0.6 mm sieve against 54.6% for the sand. Its grading curve lies in Zone III of the BS fine-aggregate limits, which points to a higher water requirement, and its particle sizes cover a wider range (uniformity coefficient 5.8 against 3.1). Sedimentation analysis (Table 3) found 14.0% clay and 22.6% silt in the laterite, which is classed as sandy clay under USCS, whereas the river sand contained 2.3% clay and 6.2% silt.

Table 2. Physical properties of the fine aggregates.

Property	River sand	Laterite
Fineness modulus	2.65	2.21
Uniformity coefficient, C_u	3.1	5.8
Passing 0.6 mm sieve (%)	54.6	72.8
Specific gravity	2.63	2.48
Natural moisture content (%)	–	8.4
Water absorption (%)	2.5	11.2

Specific gravity of the coarse aggregate and cement was 2.72 and 3.05, respectively.

Table 3. Particle-size fractions by sedimentation analysis (ASTM D422).

Material	Sand (%)	Silt (%)	Clay (%)
Abuja river sand	91.5	6.2	2.3
Lugbe laterite	63.4	22.6	14.0

The laterite's specific gravity (2.48) is below that of the river sand (2.63), in line with a more porous, clay-rich and iron-bearing particle. Together with its absorption of 11.2%, this means laterite will raise the water demand of a mix and could weaken the paste–aggregate bond if left uncontrolled, which is the reason a superplasticizer was included. The cement's specific gravity (3.05) is a little under the usual 3.10–3.16 range; storage conditions or clinker variation may explain this, and the gap is too small to affect mix proportioning appreciably.

3.2 Fresh properties

Slump flow lay between 551.29 mm (Z443) and 579.90 mm (Z223), averaging 566.2 mm over the 56 mixtures (Fig. 3c, Table A2). Every mixture therefore reached or exceeded the 550 mm lower limit of the EFNARC range [19]. The largest flows belonged to Z223, Z16 and Z114, and the smallest to Z443, Z146 and Z2. Such a narrow spread shows that the superplasticizer largely cancelled the extra water demand of the laterite fines, so workability did not decide the comparison between mixtures. The lower flows are linked to mixtures with more fines and higher absorption, which leave less free water to lubricate the mix.

3.3.1 Compressive strength

Mean compressive strength ranged from 20.28 MPa (Z34) to 26.21 MPa (Z12), with a mean of 23.09 MPa (standard deviation 1.35 MPa) over the 56 mixtures (Fig. 3a, Table A2). The highest values were obtained for Z12 (26.21 MPa), Z6 (25.96 MPa), Z13 (25.30 MPa), Z4 (25.15 MPa) and Z113 (25.14 MPa), and the lowest for Z34 (20.28 MPa), Z124 (21.10 MPa), Z15 (21.28 MPa) and Z246 (21.31 MPa).

Plausible reasons for the higher strengths of some mixtures are that fine lateritic particles occupy voids between cement grains and aggregates, increasing packing density and reducing pore connectivity, and that iron- and aluminium-bearing fines may act as nucleation sites for hydration products. In mixtures with an excess of clay-bearing

fines, higher water demand, mixing water absorbed by the clay and incomplete hydration would be expected to raise porosity and weaken the ITZ. These mechanisms are inferred from the literature and from the SEM observations in Section 3.4; the strength data alone do not separate them (Section 3.5).

The plot of compressive strength against laterite content (0–4% of the fine aggregate) prepared for the dissertation showed an overall downward trend, so within this narrow range additional laterite did not increase strength as shown in figure 2 below.

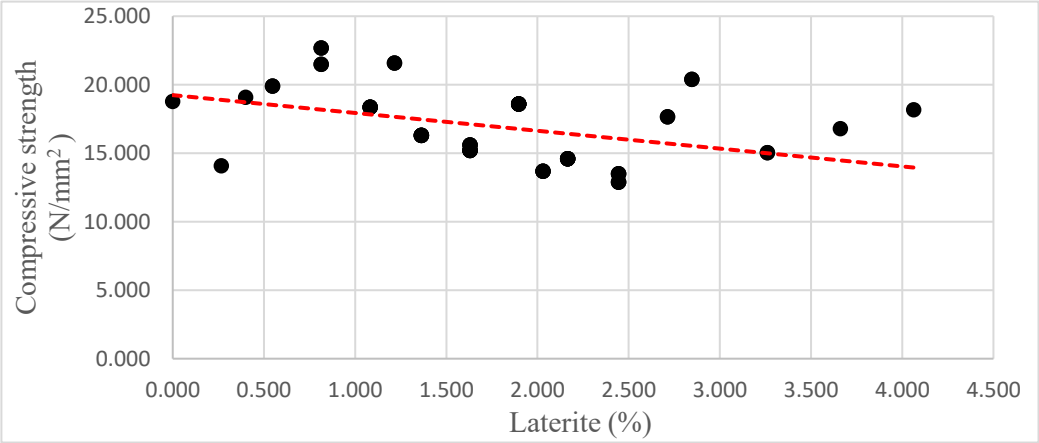

Figure 1: Relationship between laterite content and the compressive strength of concrete partially replacing sand

Scatter among replicates was considerable. The three cubes of a mixture had a mean coefficient of variation of 13% (maximum 26%), and the pooled standard deviation of compressive strength was 3.3 MPa, similar to the whole range of mixture means (20.3–26.2 MPa). Differences between neighbouring mixtures should therefore be read with care (Section 3.5).

3.3.2 Flexural strength

Mean flexural strength ranged from 2.73 MPa (Z5) to 3.80 MPa (Z225), with an overall mean of 3.24 MPa (Fig. 3b, Table A2). Other high values were found for Z45 (3.61 MPa), Z332 (3.59 MPa), Z25 (3.56 MPa) and Z1 (3.52 MPa), and low values for Z246 (2.81 MPa), Z245 (2.86 MPa), Z24 (2.89 MPa) and Z146 (2.95 MPa). Differences between mixtures were proportionally smaller than for compressive strength. The higher flexural strengths are attributed to better paste–aggregate bonding and a denser ITZ, which reduce the number of crack-starting sites and spread stress more evenly under bending; the lower values are attributed to excess lateritic fines that disturb

bonding and promote microcracking through drying and shrinkage. The pooled standard deviation of the three specimens was 0.45 MPa (about 14% of the mean).

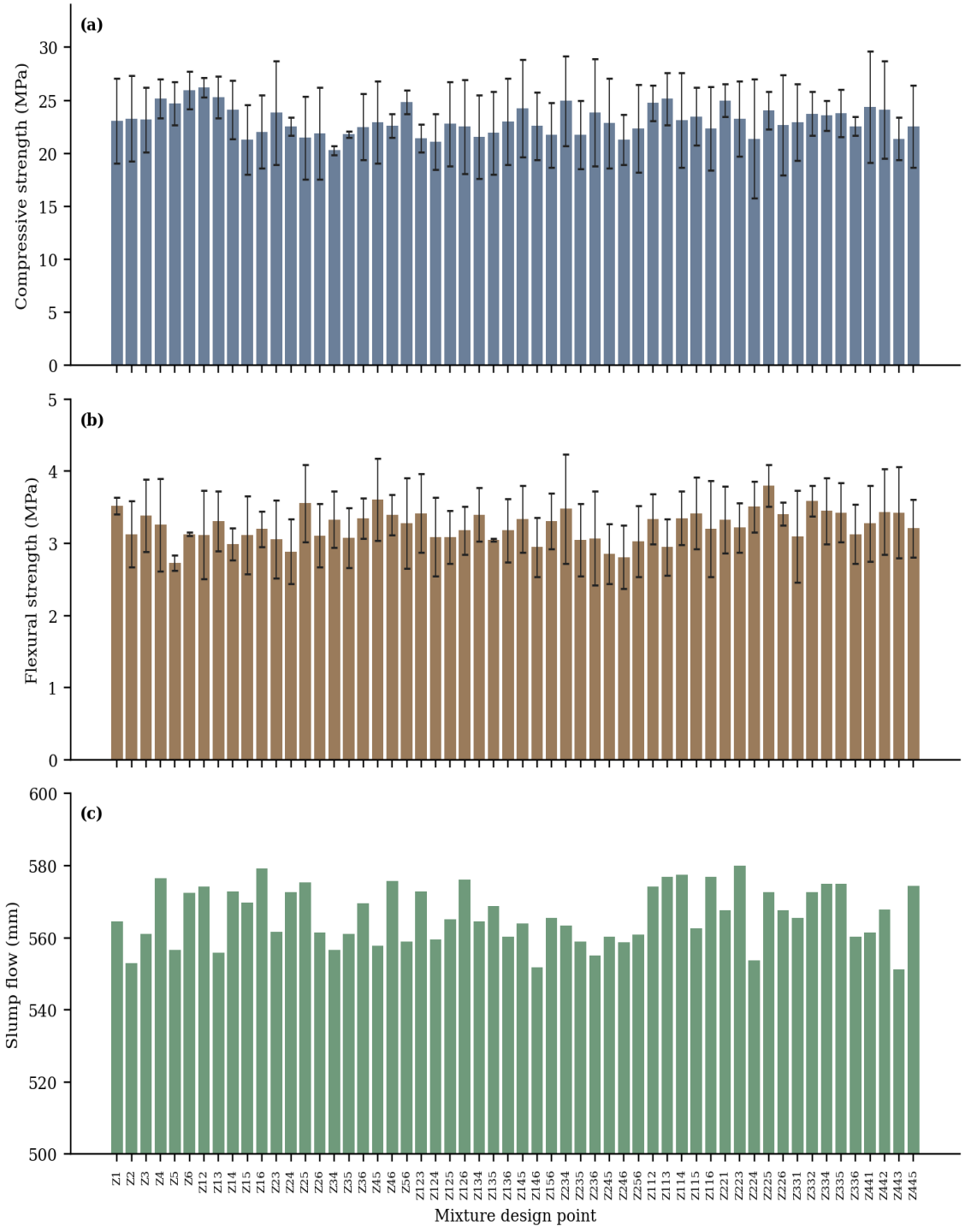

Figure.3**.** (a) Mean compressive strength, (b) mean flexural strength and (c) slump flow of the 56 mixtures. Error bars in (a) and (b) show the standard deviation of three specimens.

3.4 Microstructure (SEM–EDS)

The SEM micrographs (Fig. 4) and EDS analyses of the four selected spots are summarized in Table 4. EDS detected Ca, Si, O, Al, Fe, Mg, K and Na in all spots, as expected for a hydrated cement paste containing river sand and lateritic soil. EDS was used qualitatively, to compare the main elements present at each spot; quantitative elemental compositions were not recorded.

Spot 1 (Z12, Z6, Z4, Z221) showed a dense, homogeneous matrix of closely packed hydration products, with fibrous and foil-like C–S–H around both natural aggregate and lateritic fines. The ITZ was compact and continuous, and only a few isolated capillary pores were seen. The EDS spectrum was dominated by Ca, Si and O, with appreciable Al and Fe, indicating that the laterite took part in the hydration process without disrupting the continuity of the paste. Spot 2 (Z56, Z112, Z145, Z225, Z332, Z334) also had continuous hydration products and good ITZ adhesion, but with slightly more microvoids around lateritic particles, attributed to the higher absorption of laterite. Spot 3 (Z34, Z123, Z124, Z224, Z443) showed increased pore distribution, discontinuous hydration products, localized microcracks and a less compact ITZ, with higher Al and Fe and less Ca-rich product in the EDS spectrum. Spot 4 (Z15, Z26, Z35, Z135, Z156, Z235) was the most heterogeneous, with loosely packed hydration products, interconnected pores, microcracks extending through the paste, a discontinuous ITZ and the lowest Ca intensity.

Table 4. Mixtures represented by each SEM–EDS spot and their mean laboratory performance.

Spot	Representative mixtures	f_c (MPa)	f_{cr} (MPa)	Slump flow (mm)	Microstructure
1	Z12, Z6, Z4, Z221	25.57	3.21	573	Dense; compact ITZ
2	Z56, Z112, Z145, Z225, Z332, Z334	24.20	3.47	570	Continuous; few voids
3	Z34, Z123, Z124, Z224, Z443	21.11	3.36	559	Porous; microcracks
4	Z15, Z26, Z35, Z135, Z156, Z235	21.74	3.12	564	Heterogeneous; connected pores

Mean of the listed mixtures, calculated from Table A2.

The microstructure thus agrees with the laboratory results: the dense, C–S–H-rich matrices at Spots 1 and 2 belong to mixtures averaging 25.6 and 24.2 MPa, while the porous, microcracked matrices at Spots 3 and 4 belong to mixtures averaging 21.1 and 21.7 MPa. Spots 3 and 4 hardly differ in compressive strength, but the mixtures at Spot 4, whose microstructure is the most heterogeneous; have the lowest mean flexural strength (3.12 MPa against 3.36 MPa at Spot 3). This fits the greater microcracking and pore connectivity seen there, although the difference is small compared with specimen scatter. The spots were picked to represent higher- and lower-performing mixtures, so the contrast between groups partly reflects that choice, and the replicate scatter described in Section 3.5 makes rankings of individual mixtures uncertain. With these limits in mind, the observations support the view that laterite can work as a micro-filler where its clay content is controlled, and as a clay contaminant that increases internal water demand and weakens the ITZ where it is not. The pore networks at Spots 3 and 4 may also leave such mixtures more open to moisture ingress in service, although durability was not tested.

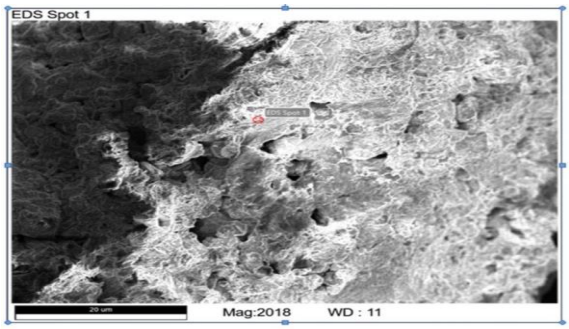

(a) Spot 1: dense hydrated mixture

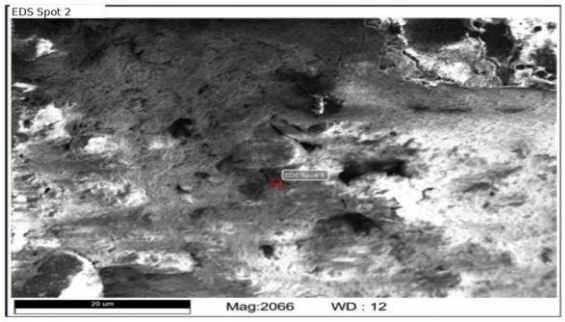

(b) Spot 2: moderate laterite mixture

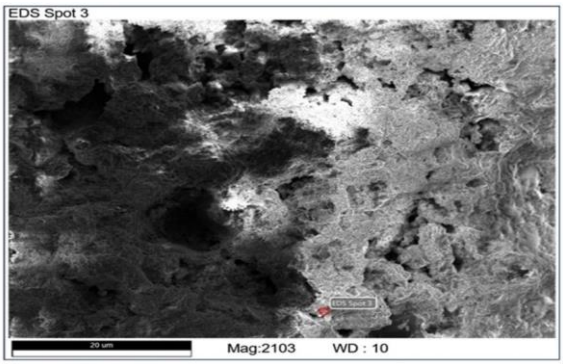

(c) Spot 3: high-laterite mixture

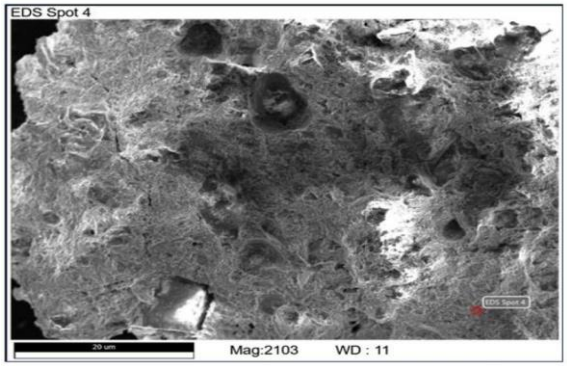

(d) Spot 4: excessive-laterite mixture

Figure 4. SEM micrographs of selected laterized concrete mixtures (magnification about 2000×, scale bar 20 µm).

3.5 Replicate analysis of variance and the Scheffé models

Because three specimens were tested per mixture, differences between mixtures can be judged against the pure error of the replicates (Table 5). For compressive strength the

between-mixture mean square (5.44) is smaller than the replicate mean square (11.00), giving $F = 0.49$ with 55 and 112 degrees of freedom ($p = 0.998$); for flexural strength the corresponding values are 0.141 and 0.204 ($F = 0.69$, $p = 0.935$). The pooled replicate standard deviations are 3.32 MPa (14% of the mean) and 0.45 MPa (14%). The experiment therefore could not detect differences between the 56 mixtures in either strength: the spread of the mixture means is of the size expected from specimen-to-specimen variability alone. The rankings of mixtures in Table A2 and the polynomial surfaces fitted to the mixture means (coefficients in Table A3) should accordingly be regarded as exploratory. The dissertation reported R^2 of 0.997 and 0.995 for the polynomials, but the reported model has 60 coefficients for 56 mixture means, and a model with as many parameters as observations fits its own data almost exactly, so R^2 is not evidence of predictive ability. The F ratios of 350 and 276 reported there could not be reproduced from the sums of squares given.

Table 5. One-way ANOVA of mixture effects using the replicate specimens (three per mixture).

Strength / source	Sum of squares	df	Mean square	*F*	*p*
Compressive					
Between mixtures	299.38	55	5.44	0.49	0.998
Within mixtures (replicates)	1232.16	112	11.00	–	–
Total	1531.55	167	–	–	–
Flexural					
Between mixtures	7.77	55	0.141	0.69	0.935
Within mixtures (replicates)	22.88	112	0.204	–	–
Total	30.64	167	–	–	–

df, degrees of freedom. Sums of squares were calculated from the individual results in Table A2.

3.6 Optimization

The dissertation reported that maximizing the fitted polynomials gave predicted strengths of about 28.46 MPa (compressive) and 4.52 MPa (flexural) at a laterite replacement of 20–30% of the fine aggregate. The best measured mixtures were Z12 (26.21 MPa compressive) and Z225 (3.80 MPa flexural), but their differences from the other mixtures are within replicate scatter. Confirming any candidate mixture requires additional specimens cast at the proposed proportions.

Table 6 lists the two best measured mixtures as practical candidates: Z12, which gave the highest mean compressive strength, and Z225, which gave the highest mean flexural strength. Both lie inside the experimental region, with laterite at no more than 4% of the fine aggregate, so neither supports a conclusion about the 20–30% replacement range.

Table 6. Candidate mixtures from the laboratory programme (mean ± standard deviation of three specimens at 28 days).

Mix	Selected for	fc (MPa)	fcr (MPa)	Slump flow (mm)	Batch quantities (kg per batch)
Z12	Highest mean compressive strength	26.21 ± 0.92	3.12 ± 0.61	574	Water 0.510, cement 0.935, river sand 2.44, laterite 0.015(0.6% of fine aggregate), superplasticizer 0.022, coarse aggregate 2.780
Z225	Highest mean flexural strength	24.05 ± 1.74	3.80 ± 0.29	573	Water 0.510, cement 0.900, river sand 2.430, laterite 0.010(0.4% of fine aggregate), superplasticizer 0.022, coarse aggregate 2.860

Strengths calculated from Table A2. Quantities are the Table A1 rows S7 (Z12) and S46 (Z225), which they are model optimum.

Confirmation is proposed as follows and has not yet been carried out. Z12 and Z225 would each be re-cast from fresh batches of the same materials, using the mixing, compaction and curing procedures of Section 2, with at least six 150 mm cubes and six 160 × 40 × 40 mm prisms per mixture, tested at 28 days. A mixture would be regarded as confirmed if the mean of the new specimens does not differ significantly (two-sample t test, 5% level) from its original three-specimen mean, and if that mean lies inside the

interval predicted by the fitted model. Because the third-degree model has as many coefficients as there are mixtures, it has no residual degrees of freedom, so this interval would have to be built from the pure-error (replicate) variance of Section 3.5. With a pooled standard deviation of 3.3 MPa, six cubes give a standard error of the mean of about 1.3 MPa, so differences of a few MPa between mixtures cannot be resolved with this number of specimens. Testing laterite at 20–30% of the fine aggregate would require new design points beyond the 4% studied here, together with their own confirmation batches.

4. CONCLUSIONS

The following conclusions come from this laboratory study of concrete in which Abuja river sand was partly replaced by Lugbe laterite:

1. The laterite is sandy clay (SiO_2 ≈ 32%, Al_2O_3 ≈ 20%, Fe_2O_3 ≈ 8%; clay fraction 14%). It is finer and more porous than the river sand (fineness modulus 2.21 against 2.65; specific gravity 2.48 against 2.63; water absorption 11.2%), and it therefore increases water demand.

2. With a superplasticizer, all 56 mixtures reached slump flows of 551–580 mm, at or above the EFNARC lower limit of 550 mm.

3. Mean compressive strength ranged from 20.28 to 26.21 MPa and mean flexural strength from 2.73 to 3.80 MPa at laterite contents up to 4% of the fine aggregate, showing that such concrete can attain low to medium structural strength levels.

4. SEM–EDS of four groups of mixtures showed dense, C–S–H-rich matrices with compact ITZs in the stronger groups, and greater porosity, interrupted hydration products and microcracks in the weaker groups. These observations are consistent with laterite acting as a micro-filler where its clay content is controlled and as a clay contaminant where it is not.

5. The variation among the three specimens of each mixture (coefficient of variation about 14%) was as large as the differences between mixtures, and replicate-based ANOVA detected no significant mixture effect on compressive strength ($p = 0.998$) or flexural strength ($p = 0.935$). The fitted Scheffé models and their predicted maxima

(28.46 and 4.52 MPa) are therefore unconfirmed, and no optimum replacement level can be stated from this programme.

6. Replacing part of the river sand with laterite could lessen dependence on river sand extraction in the FCT, provided the laterite is characterized and the mixture optimized; a larger replicated programme over a wider replacement range is needed to establish this.

Further work should use more replicate specimens, a wider replacement range (for example 0–30%) and confirmation batches. It should also cover long-term durability (chloride penetration, sulphate resistance and carbonation), strength at later ages, cost and life-cycle assessment, and the use of laterite in self-compacting and high-performance concrete.

5. RECOMMENDATIONS

1. Characterize any laterite intended as a fine-aggregate replacement before use, since its grading, clay fraction, mineralogy and water absorption differ from place to place.
2. Choose replacement levels through mix optimization instead of applying one fixed percentage to all lateritic materials.
3. Include workability, compressive strength and durability-related tests in quality control for the specific laterite source and concrete grade.
4. Validate the optimized mixture at larger scale and study long-term durability mechanisms, including permeability, chloride ingress, sulphate exposure and shrinkage.

ACKNOWLEDGEMENTS: The authors thank the staff of the Nigerian Building and Road Research Institute (NBRRI) laboratory, Jabi, Abuja, and the Department of Civil Engineering, University of Abuja.

REFERENCE

[1] L. Koehnken, M. S. Rintoul, M. Goichot, D. Tickner, A.-C. Loftus and M. C. Acreman, "Impacts of riverine sand mining on freshwater ecosystems: a review of the scientific evidence and guidance for future research," River Research and Applications, vol. 36, no. 3, pp. 362–370, 2020. doi:10.1002/rra.3586

[2] D. Adepegba, "A comparative study of normal concrete with concrete which contained laterite instead of sand," Building Science, vol. 10, no. 2, pp. 135–141, 1975. doi:10.1016/0007-3628(75)90029-8

[3] L. A. Balogun and D. Adepegba, "Effect of varying sand content in laterized concrete," International Journal of Cement Composites and Lightweight Concrete, vol. 4, no. 4, pp. 235–240, 1982. doi:10.1016/0262-5075(82)90027-6

[4] F. Lasisi and J. A. Osunade, "Factors affecting the strength and creep properties of laterized concrete," Building and Environment, vol. 20, no. 2, pp. 133–138, 1985. doi:10.1016/0360-1323(85)90008-3

[5] F. Lasisi, J. A. Osunade and A. O. Adewale, "Short-term studies on the durability of laterized concrete and laterite-cement mortars," Building and Environment, vol. 25, no. 1, pp. 77–83, 1990. doi:10.1016/0360-1323(90)90044-R

[6] F. F. Udoeyo, U. H. Iron and O. O. Odim, "Strength performance of laterized concrete," Construction and Building Materials, vol. 20, no. 10, pp. 1057–1062, 2006. doi:10.1016/j.conbuildmat.2005.03.002

[7] F. F. Udoeyo, R. Brooks, C. Utam, P. Udo-inyang and E. C. Ukpong, "Effect of non-standard curing methods on the compressive strength of laterized concrete," ARPN Journal of Engineering and Applied Sciences, vol. 5, no. 2, pp. 6–20, 2010.

[8] J. O. Ukpata and M. E. Ephraim, "Flexural and tensile strength properties of concrete using lateritic sand and quarry dust as fine aggregate," ARPN Journal of Engineering and Applied Sciences, vol. 7, no. 3, pp. 324–331, 2012.

[9] A. Adesina and K. Olusola, "Partial replacement of river sand with laterite in concrete production," International Journal of Engineering and Technology, vol. 6, no. 3, pp. 149–155, 2016.

[10] J. O. Oluremi, O. O. Adeyemi and A. O. Adebayo, "Evaluation of laterite as partial replacement for sand in concrete production," Journal of Engineering Research and Reports, vol. 8, no. 1, pp. 1–9, 2019.

[11] L. O. Ettu, K. O. Olusola and J. I. Ugwu, "Strength of laterite concrete produced with different grades of ordinary Portland cement," International Journal of Engineering and Technology, vol. 3, no. 7, pp. 686–693, 2013.

[12] K. Nandhini and S. Priya, "Experimental investigation on partial replacement of river sand with laterite in concrete," International Journal of Innovative Research in Science, Engineering and Technology, vol. 6, no. 5, pp. 8633–8640, 2017.

[13] O. Alawode and O. Idowu, "Effects of water-cement ratios on the compressive strength and workability of concrete and lateritic concrete mixes," The Pacific Journal of Science and Technology, vol. 12, no. 2, pp. 99–105, 2011.

[14] K. Scrivener, "The microstructure of concrete," in Materials Science of Concrete I, pp. 127–161, 1989.

[15] S. N. B. Gowda, C. Rajasekaran and S. C. Yaragal, "Significance of processing laterite on strength characteristics of laterized concrete," IOP Conference Series: Materials Science and Engineering, vol. 431, no. 8, 2018. doi:10.1088/1757-899X/431/8/082003

[16] P. O. Awoyera, J. O. Akinmusuru, A. R. Dawson, J. M. Ndambuki and N. H. Thom, "Microstructural characteristics, porosity and strength development in ceramic-laterized concrete," Cement and Concrete Composites, vol. 86, pp. 224–237, 2018. doi:10.1016/j.cemconcomp.2017.11.017

[17] P. O. Awoyera, A. R. Dawson, N. H. Thom and J. O. Akinmusuru, "Suitability of mortars produced using laterite and ceramic wastes: Mechanical and microscale analysis," Construction and Building Materials, vol. 148, pp. 195–203, 2017. doi:10.1016/j.conbuildmat.2017.05.031

[18] H. Scheffé, "Experiments with mixtures," Journal of the Royal Statistical Society: Series B, vol. 20, no. 2, pp. 344–360, 1958.

[19] EFNARC, Specification and Guidelines for Self-Compacting Concrete. Farnham, UK: EFNARC, 2005.

APPENDIX A. SUPPLEMENTARY TABLES

Table A1. Batch quantities (kg per batch) of the 56 mixtures (Scheffé {6,3} design).

Mix	Water (X_1)	Cement (X_2)	River sand (X_3)	Laterite (X_4)	Superplasticizer (X_5)	Coarse agg. (X_6)
S1	0.516	0.938	2.435	0.00	0.014	2.785
S2	0.50	0.90	2.40	0.10	0.020	2.80
S3	0.53	0.91	2.41	0.05	0.015	2.85
S4	0.52	0.925	2.43	0.02	0.018	2.80
S5	0.54	0.94	2.40	0.00	0.025	2.86
S6	0.505	0.915	2.42	0.03	0.022	2.79
S7	0.51	0.935	2.44	0.015	0.012	2.78
S8	0.495	0.885	2.39	0.08	0.02	2.83
S9	0.52	0.925	2.405	0.025	0.016	2.85
S10	0.53	0.94	2.415	0.01	0.018	2.86
S11	0.50	0.90	2.38	0.10	0.03	2.87
S12	0.525	0.91	2.425	0.035	0.014	2.80
S13	0.515	0.92	2.42	0.045	0.012	2.79
S14	0.505	0.905	2.44	0.02	0.02	2.78
S15	0.51	0.93	2.43	0.015	0.014	2.80
S16	0.50	0.895	2.41	0.055	0.022	2.81
S17	0.525	0.91	2.43	0.025	0.018	2.82
S18	0.515	0.925	2.40	0.035	0.016	2.83
S19	0.51	0.935	2.42	0.02	0.014	2.84
S20	0.505	0.92	2.44	0.005	0.022	2.85
S21	0.50	0.91	2.43	0.022	0.018	2.86
S22	0.515	0.935	2.42	0.015	0.012	2.87
S23	0.525	0.92	2.40	0.04	0.02	2.84

Mix	Water (X_1)	Cement (X_2)	River sand (X_3)	Laterite (X_4)	Superplasticizer (X_5)	Coarse agg. (X_6)
S24	0.53	0.915	2.41	0.03	0.016	2.83
S25	0.51	0.905	2.425	0.02	0.025	2.85
S26	0.50	0.89	2.40	0.09	0.018	2.86
S27	0.515	0.925	2.405	0.015	0.022	2.87
S28	0.525	0.93	2.39	0.005	0.02	2.85
S29	0.51	0.915	2.42	0.035	0.014	2.83
S30	0.50	0.90	2.435	0.025	0.012	2.84
S31	0.52	0.925	2.41	0.02	0.02	2.86
S32	0.53	0.91	2.42	0.015	0.014	2.85
S33	0.505	0.895	2.405	0.045	0.022	2.87
S34	0.515	0.925	2.43	0.01	0.018	2.84
S35	0.50	0.90	2.40	0.06	0.02	2.86
S36	0.51	0.93	2.42	0.005	0.025	2.83
S37	0.525	0.92	2.41	0.02	0.018	2.85
S38	0.515	0.91	2.405	0.03	0.02	2.86
S39	0.50	0.895	2.42	0.045	0.012	2.87
S40	0.52	0.925	2.43	0.015	0.025	2.84
S41	0.51	0.90	2.415	0.02	0.018	2.85
S42	0.505	0.915	2.41	0.01	0.02	2.86
S43	0.53	0.94	2.4	0.005	0.014	2.87
S44	0.50	0.91	2.42	0.035	0.018	2.84
S45	0.515	0.925	2.405	0.025	0.02	2.85
S46	0.51	0.90	2.43	0.01	0.022	2.86
S47	0.525	0.915	2.41	0.03	0.014	2.84
S48	0.50	0.895	2.42	0.045	0.025	2.85
S49	0.52	0.925	2.43	0.015	0.018	2.86

Mix	Water (X_1)	Cement (X_2)	River sand (X_3)	Laterite (X_4)	Superplasticizer (X_5)	Coarse agg. (X_6)
S50	0.51	0.91	2.405	0.025	0.02	2.84
S51	0.505	0.90	2.42	0.03	0.022	2.85
S52	0.525	0.92	2.41	0.015	0.025	2.86
S53	0.51	0.90	2.40	0.05	0.018	2.84
S54	0.50	0.91	2.43	0.02	0.022	2.85
S55	0.515	0.925	2.42	0.015	0.014	2.86
S56	0.53	0.935	2.41	0.03	0.016	2.85

Table A2. Individual and mean strengths and slump flow of the 56 mixtures.

Mix	f_c 1	f_c 2	f_c 3	f_c mean	f_{cr} 1	f_{cr} 2	f_{cr} 3	f_{cr} mean	Slump flow (mm)
Z1	20.22	27.65	21.30	23.06	3.41	3.64	3.50	3.52	564.54
Z2	26.71	24.32	18.83	23.29	3.62	2.71	3.06	3.13	552.92
Z3	20.07	26.17	23.27	23.17	3.63	3.72	2.81	3.39	561.13
Z4	27.19	23.66	24.61	25.15	3.99	2.79	3.00	3.26	576.58
Z5	22.88	24.35	26.93	24.72	2.83	2.73	2.62	2.73	556.61
Z6	24.12	26.12	27.65	25.96	3.14	3.11	3.15	3.13	572.47
Z12	25.66	27.27	25.70	26.21	3.14	2.50	3.72	3.12	574.20
Z13	23.18	27.13	25.59	25.30	2.98	3.77	3.17	3.31	555.90
Z14	20.97	26.25	25.10	24.11	3.05	2.74	3.17	2.99	572.94
Z15	19.88	18.94	25.02	21.28	3.22	3.61	2.54	3.12	569.72
Z16	18.81	21.61	25.67	22.03	3.31	3.37	2.92	3.20	579.26
Z23	25.38	18.36	27.74	23.83	2.90	3.66	2.61	3.06	561.65
Z24	22.41	23.46	21.74	22.54	2.70	3.40	2.57	2.89	572.70
Z25	19.58	25.96	18.83	21.46	2.95	3.94	3.80	3.56	575.32
Z26	26.80	18.51	20.40	21.90	2.70	3.07	3.57	3.11	561.37

Mix	f_c 1	f_c 2	f_c 3	f_c mean	f_{cr} 1	f_{cr} 2	f_{cr} 3	f_{cr} mean	Slump flow (mm)
Z34	20.74	19.89	20.21	20.28	2.98	3.25	3.75	3.33	556.71
Z35	22.14	21.65	21.64	21.81	3.52	3.01	2.70	3.08	561.05
Z36	20.96	20.44	26.10	22.50	3.40	3.61	3.05	3.35	569.58
Z45	24.29	25.95	18.60	22.95	4.00	2.95	3.87	3.61	557.72
Z46	23.80	21.52	22.50	22.61	3.34	3.70	3.15	3.40	575.75
Z56	24.00	24.39	26.13	24.84	3.32	2.63	3.89	3.28	558.86
Z123	20.66	22.93	20.64	21.41	3.46	2.85	3.94	3.42	572.92
Z124	20.85	23.83	18.63	21.10	3.59	3.16	2.51	3.09	559.63
Z125	20.54	27.39	20.42	22.78	3.42	2.69	3.15	3.09	565.13
Z126	21.28	27.44	18.85	22.52	3.38	2.80	3.37	3.18	576.23
Z134	19.44	19.12	26.08	21.55	3.41	3.76	3.02	3.40	564.56
Z135	19.66	26.44	19.70	21.93	3.03	3.06	3.06	3.05	568.73
Z136	27.64	21.46	19.95	23.02	3.67	2.83	3.03	3.18	560.28
Z145	27.60	19.01	26.15	24.25	3.41	3.77	2.85	3.34	564.06
Z146	19.88	21.83	26.10	22.60	2.96	3.36	2.54	2.95	551.84
Z156	18.24	23.10	23.89	21.74	2.87	3.45	3.60	3.31	565.59
Z234	20.05	27.61	27.15	24.94	2.61	3.83	4.00	3.48	563.47
Z235	25.00	21.72	18.60	21.77	3.02	3.57	2.56	3.05	558.97
Z236	25.80	18.12	27.65	23.86	2.52	2.90	3.79	3.07	555.19
Z245	18.23	26.60	23.71	22.85	2.75	2.51	3.32	2.86	560.22
Z246	23.78	19.11	21.03	21.31	2.59	3.32	2.53	2.81	558.85
Z256	18.02	22.78	26.26	22.35	2.92	3.56	2.60	3.03	560.88
Z112	23.15	26.50	24.59	24.75	3.02	3.71	3.29	3.34	574.26
Z113	24.40	23.15	27.87	25.14	3.39	2.79	2.66	2.95	576.87
Z114	27.86	22.47	19.07	23.13	3.66	3.45	2.94	3.35	577.45
Z115	20.59	26.00	23.81	23.47	3.44	3.91	2.91	3.42	562.65

Mix	f_c **1**	f_c **2**	f_c **3**	f_c **mean**	f_{cr} **1**	f_{cr} **2**	f_{cr} **3**	f_{cr} **mean**	**Slump flow (mm)**
Z116	26.02	18.20	22.73	22.33	2.74	2.89	3.96	3.20	576.95
Z221	26.70	23.73	24.52	24.98	3.84	2.94	3.20	3.33	567.61
Z223	27.23	22.11	20.42	23.25	3.60	3.14	2.93	3.22	579.90
Z224	18.02	27.85	18.31	21.39	3.25	3.36	3.91	3.51	553.73
Z225	22.69	26.01	23.44	24.05	3.47	3.99	3.95	3.80	572.70
Z226	27.81	18.54	21.65	22.67	3.26	3.38	3.58	3.41	567.65
Z331	21.99	19.90	26.92	22.94	2.75	3.83	2.71	3.10	565.44
Z332	26.14	22.52	22.59	23.75	3.46	3.48	3.83	3.59	572.75
Z334	23.46	25.03	22.19	23.56	3.98	3.21	3.16	3.45	575.00
Z335	25.71	21.32	24.33	23.79	3.66	2.96	3.68	3.43	574.93
Z336	22.85	21.60	23.26†	22.57	2.77	3.03	3.58	3.13	560.32
Z441	18.29	27.21	27.61	24.37	2.68	3.67	3.48	3.28	561.42
Z442	18.87	27.54	25.89	24.10	3.90	2.77	3.65	3.44	567.86
Z443	19.11	22.08	22.97	21.39	3.87	2.71	3.72	3.43	551.29
Z445	20.51	26.99	20.11	22.53	3.62	2.82	3.19	3.21	574.44

f_c, compressive strength (MPa); f_{cr}, flexural strength (MPa).

Table A3. Regression coefficients of the Scheffé third-degree models, as presented in the dissertation.

Term	f_c **coeff.**	f_{cr} **coeff.**
β_1	21.376	2.743
β_2	19.22	-0.082
β_3	17.95	3.188
β_4	20.1	3.335
β_5	19.5	2.697
β_6	21.0	4.027
β_{12}	11.456	1.987
β_{13}	-1.442	2.336
β_{14}	-4.015	3.404
β_{15}	12.515	2.741
β_{16}	9.769	2.541
β_{23}	17.871	-0.956
β_{24}	1.884	1.971
β_{25}	-1.919	-1.965
β_{26}	2.705	2.089
β_{34}	3.147	1.45
β_{35}	-0.899	-0.967
β_{36}	3.863	2.743
β_{45}	11.989	1.601
β_{46}	8.09	2.488
β_{56}	-1.8	-2.639
β_{123}	10.613	5.073
β_{124}	9.237	1.883
β_{125}	3.732	2.11

Term	**f_c coeff.**	**f_{cr} coeff.**
β_{126}	7.068	1.574
β_{134}	-2.757	3.409
β_{135}	21.376	2.245
β_{136}	9.241	1.458
β_{145}	4.617	3.856
β_{146}	6.626	0.886
β_{156}	12.265	2.25
β_{234}	6.851	0.094
β_{235}	3.824	4.168
β_{236}	8.415	2.941
β_{245}	11.547	4.356
β_{246}	-2.697	4.116
β_{256}	4.81	1.604
β_{345}	16.967	1.483
β_{346}	-2.455	-1.562
β_{356}	10.03	1.579
β_{456}	17.326	2.697
β_{112}	-18.838	-2.64
β_{113}	15.227	1.59
β_{114}	-5.67	-0.027
β_{115}	8.557	1.375
β_{116}	2.134	2.677
β_{221}	-1.924	2.335
β_{223}	-0.944	3.942
β_{224}	3.839	1.986

Term	**f_c coeff.**	**f_{cr} coeff.**
β_{225}	6.216	0.637
β_{226}	11.046	0.932
β_{331}	5.587	3.705
β_{332}	4.872	2.072
β_{334}	2.901	1.145
β_{335}	-5.661	2.839
β_{336}	8.482	1.33
β_{441}	4.515	1.524
β_{442}	6.29	1.147
β_{443}	8.238	1.25
β_{445}	2.862	1.906